Electrophonon resonance in cylindrical quantum wires

SeGi Yu, V. B. Pevzner, and K. W. Kim
Department of Electrical and Computer Engineering, North Carolina State University, Raleigh, North Carolina 27695-7911

Michael A. Stroscio
U.S. Army Research Office, P.O. Box 12211, Research Triangle Park, North Carolina 27709-2211

(Received 26 February 1998)

The electrophonon resonances (EPR) in cylindrical quantum wires are investigated in the presence of confined optical phonons. A comparison with the bulk phonons reveals a sharp difference between the selection rules that apply to the bulk and confined/interface phonons. This raises a possibility of detecting phonon confinement experimentally by utilizing EPR effects.
[S0163-1829(98)10731-2]

The physics of the electrophonon resonance (EPR) is associated with the singular nature of the electron density of states in one-dimensional (1D) systems. Whenever the difference between two electron energy levels is equal to the phonon energy, and provided that the voltage bias is sufficiently high ($V>\hbar\omega_0/e$), there exists a condition for EPR.[1] The same sort of singular behavior is also typical for 3D electrons in a strong magnetic field. The resonances that arise in such systems are known as the magnetophonon resonances.[2]

The term EPR was first introduced by Bryskin and Firsov,[3] who had predicted EPR for nondegenerate bulk electron systems in strong electric fields (cf. Refs. 4 and 5). Although the resonances are achieved by the variation of the electric voltage for the cases of both Refs. 1 and 3, the nature of the underlying physics is quite different. In the case of Gurevich *et al.*[1] as well as the present study, such a voltage can be either the bias voltage across the nanowire or the gate voltage controlling the electron confinement.

Previous studies of EPR in nanostructures have considered only the effects of the bulk phonons on EPR. It is well known that the presence of heterointerfaces affects the characteristic phonon modes, resulting in confinement of both optical[6] and acoustic phonons.[7] In this paper, we investigate EPR in cylindrical quantum wires and examine the effects of *optical phonon confinement*. We focus our attention on the difference in the selection rules in order to examine a possibility of detecting phonon confinement by utilizing the EPR phenomena in quantum wires. A macroscopic dielectric continuum model[8–10] is used to describe confined and interface optical phonons. The results are compared with those of bulk phonons.

We consider an EPR configuration where two electron reservoirs are connected by a long cylindrical quantum wire of radius R and length L. Initially the chemical potentials of the two reservoirs are both equal to μ. An application of a bias voltage (V) changes the chemical potentials of the reservoirs, thus introducing a drop from $\mu+eV/2$ to $\mu-eV/2$ along the direction of the applied voltage. In the absence of scattering, electron current flows ballistically from the contact with a higher chemical potential to that with a lower one. At low bias, this current is described by the Landauer formula.[11] The conductance G is a steplike function. The height of each step is equal to the quantum conductance $G_0=2e^2/H$ scaled by a prefactor whose physical interpretation is that of a transmission probability.[11] An addition of each new step signals on ''opening'' of a new conductance channel.

With an increasing bias voltage V, one could expect a non-Ohmic behavior of the conductance. A substantial deviation of current from the Ohmic value may be expected if the ratio eV/μ is not small—cf. Ref. 12. When the effects of carrier-phonon interactions are considered, the EPR current (i.e., the amount that deviates from the ballistic current due to the EPR) in a wire is given as a sum of individual intersubband currents:[1,13]

$$\begin{aligned} J_{\mathrm{EPR}} &= \sum_{nn'} J_{\mathrm{EPR},nn'} \\ &= -\sum_{nn'} 2eL(1-e^{-\beta eV}) \int_{-\infty}^{0} \frac{dk'}{2\pi} \frac{2\pi}{\hbar} \\ &\quad \times \sum_{\mathbf{q}} |\langle n'|H'|n\rangle|^2 (\mathcal{A}^{(+)}+\mathcal{A}^{(-)})\,\delta(E'-E-\hbar\omega_{\mathbf{q}}). \end{aligned} \tag{1}$$

Here, $\beta=1/k_BT$, k_B is the Boltzmann constant, H' is the electron-phonon interaction Hamiltonian, and

$$\begin{aligned} \mathcal{A}^{(\pm)} &= -[\tfrac{1}{2}\mp\tfrac{1}{2}-f(E'-\mu^{(\pm)})][\tfrac{1}{2}\pm\tfrac{1}{2}-f(E-\mu^{(\mp)})] \\ &\quad \times(\tfrac{1}{2}\pm\tfrac{1}{2}+N_{\mathbf{q}}), \end{aligned} \tag{2}$$

where $\mu^{(\pm)}$ is equal to $\mu\pm eV/2$, f is a Fermi-Dirac distribution function, N is a Bose-Einstein function, k' is the z-directional electron wave vector (parallel to the direction of the wire), and $\mathbf{q}$ is the phonon wave vector. The summation over all the phonon branches is implicit. The term proportional to $\mathcal{A}^{(+)}$ describes phonon emission, whereas $\mathcal{A}^{(-)}$ corresponds to absorption processes. The electron energy E is expressed as $E=E(n,k)$, where n $(=l,j)$ is the cumulative index of quantum numbers. In the extreme quantum limit,

electron energies and wave functions for a cylindrical quantum wire can be represented in cylindrical coordinates (r,ϕ,z) as

$$E=E(l,j;k)=E(l,j;k=0)+\frac{\hbar^2k^2}{2m^*}$$
$$=\frac{\hbar^2}{2m^*R^2}\,[(X_j^l)^2+(kR)^2], \tag{3}$$

$$\langle \mathbf{r}|l,j;k\rangle=\frac{1}{\sqrt{\pi R^2}Y_j^l}\,J_l\left(X_j^l\,\frac{r}{R}\right)e^{il\phi}\,\frac{e^{ikz}}{\sqrt{L}}, \tag{4}$$

where $l=0,1,2,...$, $j=1,2,3,...$, X_j^l is the jth zero of the lth-order Bessel function of first kind $J_l(x)$; i.e., $J_l(X_j^l)=0$, and $Y_j^l=J_{l+1}(X_j^l)$. As expected, $J_{\rm EPR}$ diminishes the total current.

Detailed balance guarantees a vanishing EPR contribution for the equilibrium distribution function when both the temperature and the chemical potential are constant. As a result, the distribution function f gives a finite contribution to the collision, if and only if the z components of the electron initial and final wave vectors (k' and k) are of opposite sign; i.e., their chemical potentials are different. This means that the only nonzero contribution to the dissipative current is due to the phonons that backscatter the electrons, requiring the integration range for k' to shrink to a half space in Eq. (1). In low-impurity polar semiconductor materials, the Fröhlich interaction (i.e., the electron–polar-optical-phonon interaction) is the most important scattering mechanism. Therefore, we limit the focus of this study to EPR effects that are due to the Fröhlich interaction. However, the method employed here can be easily extended to include other interactions as well.

The Fröhlich Hamiltonian for bulk phonon modes is given by

$$H'_{\rm bulk}=\left[\frac{2\pi}{V}\,e^2\hbar\omega_0\left(\frac{1}{\epsilon_\infty}-\frac{1}{\epsilon_s}\right)\right]^{1/2}\sum_{\mathbf{q}}\;\frac{1}{|\mathbf{q}|}\,e^{-i\mathbf{q}\cdot\mathbf{r}}(\hat{a}_{\mathbf{q}}+\hat{a}^\dagger_{-\mathbf{q}}), \tag{5}$$

where V is the volume of the quantum wire ($V=\pi R^2L$), ω_0 is the longitudinal-optical phonon frequency, and ϵ_∞ (ϵ_s) is the high-frequency (static) dielectric constant for the quantum wire material. From Eq. (1), the EPR current for the bulk phonon case is

$$J_{\rm EPR}=-J_L\sum_{l',j'}\;\sum_{l,j}\;\sum_i\;e^{-\beta eV/2}\,\sinh(\beta eV/2)\,\delta_{l,l'}\delta_{-k'+k+q,0}$$
$$\times\int d(k'R)\int d(qR)\,\delta(qR-q_iR)\int d(q_\perp R)(q_\perp R)$$
$$\times\frac{|F^{\rm bulk}_{l'j'lj}(q_\perp R)|^2}{(qR)^2+(q_\perp R)^2}\,(\mathcal{A}^{(+)}+\mathcal{A}^{(-)})\,\frac{1}{|kR|}, \tag{6}$$

where

$$J_L=\left[2e\,\frac{\hbar\omega_0}{\pi\hbar^3}\,e^2\left(\frac{1}{\epsilon_\infty}-\frac{1}{\epsilon_s}\right)m^*\right]L, \tag{7}$$

$$F^{\rm bulk}_{l'j',lj}(\eta)=\frac{2}{Y^{l'}_{j'}Y^l_j}\int_0^1 d\xi\;\xi J_{l'}(X^{l'}_{j'}\xi)J_l(X^l_j\xi)J_0(\eta\xi). \tag{8}$$

The wave vector of the scattered electron, which satisfies the conservation of the quasimomentum, is given by

$$kR=k'R+qR$$
$$=\left(\frac{2m^*R^2}{\hbar^2}\right)^{1/2}\left(E(l',j';0)-E(l,j;0)-\hbar\omega_0+\frac{\hbar^2k'^2}{2m^*}\right)^{1/2}. \tag{9}$$

For simplicity, we ignore the dispersion of bulk optical phonons; i.e., we assume $\omega_{\mathbf{q}}=\omega_0$. In our calculations, the Bessel function identity $e^{\pm ix\cos\theta}=J_0(x)+2\Sigma_j(\pm i)^j\times J_j(x)\cos(j\theta)$ is used and only the J_0 term in the $e^{i\mathbf{q}\cdot\mathbf{r}}$ expansion survives.

For an accurate description of EPR in quantum wires, the bulk Fröhlich Hamiltonian given in Eq. (5) needs to be modified. At the heterointerface, where the phonon energy difference between the long-wavelength optical phonons of the two materials is quite large, the optical phonons of each region cannot propagate into the other region. Such penetrating phonon modes decay within a few monolayers of the heterointerface. This type of phonon is called a confined phonon.[9,10] There is another kind of a phonon mode as well, which is localized at the interface. It is called the interface (IF) phonon.[9,10] Since the dimensions of the quantum wires used in our EPR studies are sufficiently large relative to the lattice spacing, we use a macroscopic dielectric continuum model[8,9] to describe phonon confinement effects in this paper.

The Fröhlich Hamiltonian for confined phonon modes is given by[8]

$$H'_{\rm conf}=\sum_{q,m,n}\left[2\pi\hbar\left(\frac{1}{\epsilon_\infty}-\frac{1}{\epsilon_s}\right)\right]^{1/2}\sqrt{\omega_0}L\;\frac{1}{\sqrt{\pi R^2}Y_n^m}$$
$$\times\frac{1}{\sqrt{q^2+(X_n^m/R)^2}}\,J_m\left(X_n^m\,\frac{r}{R}\right)$$
$$\times e^{im\phi}e^{iqz}[\hat{a}_{mn}(q)+\hat{a}^\dagger_{mn}(q)]. \tag{10}$$

The EPR current for the confined phonons is given by

$$J_{\rm EPR}=-J_L\sum_{l',j'}\;\sum_{l,j}\;\sum_{m,n}\;\sum_i\;2e^{-\beta eV/2}\,\sinh(\beta eV/2)$$
$$\times\delta_{m,l'-l}\delta_{-k'+k+q,0}\int d(k'R)$$
$$\times\int d(qR)\,\frac{1}{|Y_n^m|^2}\,\frac{|F^{\rm conf}_{l'j'lj}(qR)|^2}{R^2(q^2+q_{mn}^2)}\,(\mathcal{A}^{(+)}+\mathcal{A}^{(-)})$$
$$\times\frac{\delta(qR-q_iR)}{|kR|}, \tag{11}$$

where $q_{mn}=X_n^m/R$ and

$$F^{\mathrm{conf}}_{l',j',l,j}(\eta)=\frac{2}{Y^{l'}_{j'}Y^{l}_{j}}\int_0^1 d\xi\ \xi J_{l'}(X^{l'}_{j'}\xi)J_{l}(X^{l}_{j}\xi)J_{l'-l}(\eta\xi). \tag{12}$$

For the resonant situation, the energy difference between the bottoms of two electron subband levels—(l_i,j_i) and (l_f,j_f)—is equal to the phonon energy, i.e., $E(l_i,j_i;k=0)-E(l_f,j_f;k=0)=\hbar\omega_0$. The transitions between the other subbands are nonresonant. Furthermore, in order for EPR to occur, the initial state must be occupied, i.e., $E(l_i,j_i;0)>\mu+eV/2$, while the final state must be vacant. This can be realized by adjusting the applied bias voltage between the reservoirs. We can calculate the resonant voltage V_r required for EPR to occur in terms of the electron subband energies, chemical potential, and optical-phonon energy; that is,

$$V_r=\frac{2}{e}[E(l_i,j_i;0)-\mu]=\frac{2}{e}[E(l_f,j_f;0)+\hbar\omega_0-\mu]. \tag{13}$$

Our numerical results are obtained for GaAs quantum wires. The EPR currents due to interactions with the bulk and confined phonons are calculated as functions of applied voltage and radius with $\hbar\omega_0=36.25$ meV, $\epsilon_\infty=10.89\epsilon_0$, $\epsilon_s=13.18\epsilon_0$, and $m^*=0.067m_0$.[14] m_0 is the electron rest mass and ϵ_0 is the dielectric constant for vacuum. The chemical potential is taken to be 15 meV and the temperature is assumed to be very low ($k_BT=1$ meV) in this calculation.

The EPR characteristics are largely affected by electron and phonon statistics through the $\mathcal{A}^{(\pm)}$ terms given by Eq. (2). At low temperature, the phonon occupation number N is negligibly small; therefore, the $\mathcal{A}^{(+)}$ term is dominant over the $\mathcal{A}^{(-)}$ term. Since J_{EPR} depends linearly on the quantum wire length L through J_L, we have normalized the currents by J_L (i.e., J_{EPR}/J_L) to eliminate the dependence on arbitrary choices.

Figure 1 shows the EPR currents for two values of radius as a function of applied voltage. Solid (dashed) lines denote the results with confined (bulk) phonons. The upper two curves of this figure correspond to the resonant cases for both the confined and bulk phonons with a significant enhancement in EPR currents. The lower curves represent the nonresonant cases. It is worthwhile to note that the EPR phenomenon is extremely sensitive to the change in confinement radius. A 1% change of radius results in a significantly reduced EPR current.

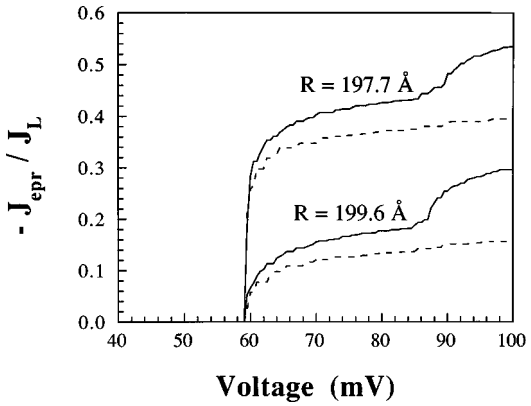

FIG. 1. EPR current vs applied voltage between two reservoirs for bulk phonons and confined phonons with the resonant case for the radius of 197.7 Å and the nonresonant case for the radius of 199.6 Å (which is 1% larger than 197.7 Å). Chemical potential is taken to be 15 meV and temperature, k_BT, is 1 meV. Solid (dashed) lines correspond to the confined (bulk) phonon case.

We also calculated EPR currents with the lowest modes of IF phonons, although the detailed derivations are not presented. The EPR current due to the IF phonon is too small to be visible for the linear scale of Fig. 1. The EPR currents for the IF phonon are roughly several (four to five) orders smaller than those for the bulk and the confined phonons. This can be understood easily since the IF phonons are localized near the radial boundaries of the wire and, accordingly, IF phonons are more important for extremely narrow quantum wires. Therefore, in a case when a wire has a radius of a few hundred angstroms, there is little interaction between the electrons—which are confined in the wire—and the IF phonons—which are localized primarily at the quantum wire boundaries. Furthermore, the extreme quantum limit used for the electron states leads to underestimates of the electron interactions with IF phonons as a result of the truncation of the electron wave functions outside the quantum wire.

Figure 2 depicts EPR currents with confined phonons for three different cases: (A) nonresonant ($R=220.0$ Å), (B) resonant where the resonant voltage is equal to the onset voltage ($R=118.7$ Å), and (C) resonant where the resonant voltage is not equal to the onset voltage ($R=340.0$ Å). The onset voltage at which electron currents start to flow to the lowest subband is given by

$$V_{\mathrm{on}}=\frac{2}{e}[E(l'',j'';0)-\mu]=\frac{2}{e}[E(l_0,j_0;0)+\hbar\omega_0-\mu], \tag{14}$$

where the subband quantum number (l_0,j_0) represents the ground state; i.e., $l_0=0$, $j_0=1$, and (l'',j'') represents any excited state with energy greater than $\hbar\omega_0$ above the ground state. For case (B), the two subbands (l_0,j_0) and (l'',j'') coincide with the resonant subbands (l_i,j_i) and (l_f,j_f), respectively, while the two sets of electron subbands do not coincide for case (C). The rapid increase for $R=340.0$ Å near 72.6 meV corresponds to a resonant transition between

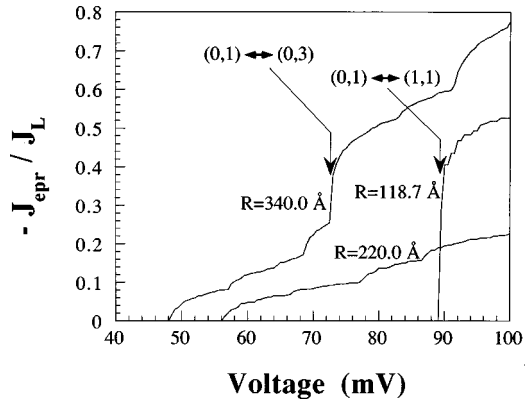

FIG. 2. EPR current vs voltage for various radii (resonant cases: 340.0 and 118.7 Å, nonresonant case: 220.0 Å). Confined phonons are used in these calculations. The arrows indicate the resonances with participating electron subband quantum numbers. Chemical potential and temperature are the same as in Fig. 1.

TABLE I. Values for resonant radius, resonant voltage, electron states involved in the resonance, onset voltage, and electron states involved in transitions at onset voltage for the two types of transitions corresponding to cases (B) and (C).

Type	Resonant radius (Å)	Resonant electron states (l,j)	Resonant voltage (meV)	Electron states at onset (l,j)	Onset voltage (meV)
B	118.7	$(0,1)\leftrightarrow(1,1)$	89.1	$(0,1)\leftrightarrow(1,1)$	89.1
B	197.7	$(0,1)\leftrightarrow(0,2)$	59.4	$(0,1)\leftrightarrow(0,2)$	59.4
B	330.7	$(0,1)\leftrightarrow(0,3)$	48.5	$(0,1)\leftrightarrow(0,3)$	48.5
C	340.0	$(0,2)\leftrightarrow(1,3)$	72.6	$(0,1)\leftrightarrow(0,2)$	47.8

two resonant states $(l_i,j_i)=(1,3)$ and $(l_f,j_f)=(0,2)$. Table I summarizes the relations between the resonant radius, resonant voltage, onset voltage, and resonant transition subbands for the two types of transitions corresponding to cases (B) and (C).

The most distinctive differences between bulk and confined phonons are the selection rules. Electron intersubband transitions between different l quantum numbers are forbidden for the case of bulk phonons, but they are allowed for the case of confined phonons [Eqs. (6) and (11)]. From the resonant condition, we can easily obtain the radius at which resonances can occur:

$$R=\left(\frac{\hbar^2}{2m^*\hbar\omega}\left[(X_{j_f}^{l_f})^2-(X_{j_i}^{l_i})^2\right]\right)^{1/2}. \tag{15}$$

Figure 3 shows how the EPR current changes as a function of radius when the applied voltage is fixed at 100 meV. The confined phonons exhibit a peak near 119 Å, which is due to the transition between the electron states of quantum number $(l,j)=(0,1)$ and $(1,1)$, whereas a bulk-phonon resonance transition is forbidden by its selection rules. This property facilitates the design of experiments that clearly separate confined and bulk phonon effects that influence electron-phonon transport. These characteristics are not altered by adopting a finite quantum-barrier potential for the electron instead of the infinite quantum barrier, since a different potential for the electron only changes both the resonant electron subband energies and the resonant radius but not the selection rule itself.

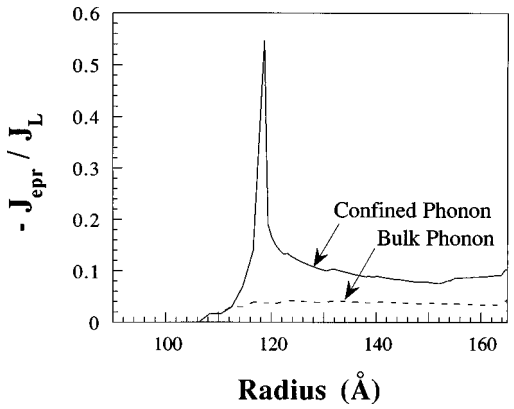

FIG. 3. EPR current vs radius for a fixed voltage ($V=100$ mV). The sharp peak at 118.7 Å indicates the resonance between the electron subbands (0,1) and (1,1) for the confined phonon, while the resonance for the bulk phonon at this radius is prohibited by the selection rule. Chemical potential and temperature are the same as in Fig. 1.

In summary, we have studied EPR phenomena in cylindrical quantum wires. The results show that EPR is controlled by changing the confinement radius and there exist three types of EPR (one nonresonant and two resonant types). We have compared the EPR with two phonon representations—bulk phonon and confined-IF phonon—and found that different selection rules apply to these two cases. We suggest that electron transport experiments can determine if the confined-IF representation is a more appropriate treatment than the bulk phonon representation. This will be an interesting and novel test since phonon confinement is usually measured experimentally by optical methods such as Raman scattering.

The authors gratefully acknowledge many discussions with Professor G. J. Iafrate. This work was supported, in part, by the U.S. Army Research Office and the Office of Naval Research.

[1] V. L. Gurevich, V. B. Pevzner, and G. Iafrate, Phys. Rev. Lett. **75**, 1352 (1995).
[2] V. L. Gurevich and Yu. A. Firsov, Zh. Eksp. Teor. Fiz. **40**, 198 (1961) [Sov. Phys. JETP **13**, 137 (1961)].
[3] V. V. Bryskin and Yu. A. Firsov, Zh. Eksp. Teor. Fiz. **61**, 2373 (1972) [Sov. Phys. JETP **34**, 1272 (1972)].
[4] D. Jovanovic, J.-P. Leburton, K. Ismail, J. M. Bigelow, and M. H. Degani, Appl. Phys. Lett. **62**, 2824 (1993).
[5] W. Xu, F. M. Peeters, and J. T. Devreese, Phys. Rev. B **48**, 1562 (1993).
[6] M. A. Stroscio, G. J. Iafrate, H. O. Everitt, K. W. Kim, Y. Sirenko, S. Yu, M. A. Littlejohn, and M. Dutta, in *Properties of III-V Quantum Well and Superlattices*, edited by P. Bhattacharya (INSPEC, The Institute of Electrical Engineers, London, 1996), p. 194.
[7] S. Yu, K. W. Kim, M. A. Stroscio, G. J. Iafrate, and A. Ballato, J. Appl. Phys. **80**, 2815 (1996).
[8] X. F. Wang and X. L. Lei, Phys. Rev. B **49**, 4780 (1994).
[9] N. Mori and T. Ando, Phys. Rev. B **40**, 6175 (1989).
[10] R. Chen, D. L. Lin, and T. F. George, Phys. Rev. B **41**, 1435 (1990).
[11] R. Landauer, IBM J. Res. Dev. **1**, 233 (1957); **32**, 306 (1989).
[12] L. P. Kouwenhoven, B. J. van Wees, C. J. P. M. Harmans, J. G. Williamson, H. van Houten, C. W. Beenakker, C. T. Foxon, and J. J. Harris, Phys. Rev. B **39**, 8040 (1989).
[13] V. L. Gurevich, V. B. Pevzner, and K. Hess, Phys. Rev. B **51**, 5219 (1995).
[14] S. Adachi, J. Appl. Phys. **58**, R1 (1985).